

# Generation of warm dense matter using an argon based capillary discharge laser



A.K. Rossall\*, G.J. Tallents

York Plasma Institute, University of York, Heslington YO10 5DD, UK

## ARTICLE INFO

### Article history:

Received 14 April 2015

Accepted 14 April 2015

Available online 23 April 2015

### Keywords:

EUV laser

High-energy-density matter

Atomic physics

Hydrodynamic modelling

Strongly coupled plasma

## ABSTRACT

Argon based capillary discharge lasers operating in the extreme ultra violet (EUV) at 46.9 nm with output up to 0.5 mJ energy per pulse and repetition rates up to 10 Hz are capable of focused irradiances of  $10^9$ – $10^{12}$  W cm<sup>-2</sup> and can be used to generate plasma in the warm dense matter regime by irradiating solid material. To model the interaction between such an EUV laser and solid material, the 2D radiative-hydrodynamic code POLLUX has been modified to include absorption via direct photo-ionisation, a super-configuration model to describe the ionization-dependent electronic configurations and a calculation of plasma refractive indices for ray tracing of the incident EUV laser radiation. A simulation study is presented, demonstrating how capillary discharge lasers of 1200 ps pulse duration can be used to generate warm dense matter at close to solid densities with temperatures of a few eV and energy densities up to  $1 \times 10^5$  J cm<sup>-3</sup>. Plasmas produced by EUV laser irradiation are shown to be useful for examining the properties of warm dense matter as, for example, plasma emission is not masked by hotter, less dense plasma emission that occurs with visible/infra-red laser target irradiation.

© 2015 Elsevier B.V. All rights reserved.

## 1. Introduction

Considerable advances have been made in higher fluence EUV and x-ray laser technology as demonstrated by free-electron lasers [1,2] and capillary discharge lasers [3,4]. With higher fluences now available, EUV and x-ray lasers can be used to directly generate strongly coupled plasmas. These plasmas are produced by irradiating solid targets with EUV/x-ray lasers, heating the sample via direct photo-ionization, resulting in typically lower temperatures and higher densities than the traditional laser produced plasma, generated using infra-red, optical and UV pulses. By reducing the wavelength into the EUV/x-ray region, the photon energy,  $E_p$ , becomes sufficient to directly photo-ionise elemental components, transferring a set amount of energy ( $E_p - E_i$ ) to the ejected electron. Reducing the lasing wavelength to the EUV/soft x-ray region allows for a tighter focus (due to a reduction in the diffraction limit) and enables the laser to penetrate into the solid material, as the critical density at these wavelengths is typically higher than solid. Due to

the unique properties of plasmas generated by EUV/x-ray lasers, these plasmas can contribute to our understanding of warm dense matter. The ability to couple a correct equation-of-state with an accurate model of radiation transport is essential in order to achieve inertial confinement fusion as the pre-ignition fuel is in the warm dense matter regime.

To promote research and to accelerate the development of industrial applications, there has been significant motivation to produce compact and affordable EUV/x-ray sources for use in parallel with large scale facilities such as the free-electron laser FLASH [5] based at DESY. The research group at Colorado State University (CSU) has developed a table-top size soft x-ray laser system [6–8] based upon capillary discharge excitation of an Ar gas producing large soft x-ray amplification.

The work presented here utilises a novel combination of 2D fluid code modelling (POLLUX) with a rapid atomic physics algorithm to simulate the EUV/x-ray interaction with solid material, the expected energy deposition within the target, the produced plasma parameters and the subsequent ablative flow away from the target. A simulation study is presented to demonstrate the capability of EUV capillary discharge lasers for the generation of warm dense matter.

\* Corresponding author.

E-mail address: [andrew.rossall@york.ac.uk](mailto:andrew.rossall@york.ac.uk) (A.K. Rossall).

## 2. POLLUX

### 2.1. Hydrodynamic code

The 2D Eulerian hydrodynamic code POLLUX [9,10], written at the University of York, was originally developed to model moderate irradiance ( $\geq 10^{10}$  W cm $^{-2}$ ) laser irradiation of a solid target producing a strongly ionized plasma which further interacts with the incident laser beam. The code solves the three first-order quasi-linear partial differential equations of hydrodynamic flow using the flux corrected transport model of Boris and Book [11] with an upwind algorithm [12] for the first term. Energy is absorbed by the plasma electrons through inverse bremsstrahlung and direct photo-ionization that is then redistributed through electron-ion collisions. The energy transfer rate between the electrons and ions is calculated using the smaller value of the Spitzer plasma collision frequency [13] or the electron-phonon collision frequency [14]. For calculation of the equation-of-state (EOS) variables, POLLUX utilizes in-line hydrodynamic EOS subroutines from the Chart-D [15] equation-of-state package developed at Sandia National Laboratories. As POLLUX uses an explicit solver, a maximum Courant number of  $C \sim 1$  is required. When accounting for both spatial directions the Courant number is given by,

$$C = \frac{u_x \Delta t}{\Delta x} + \frac{u_y \Delta t}{\Delta y} \sim 1. \quad (1)$$

Here  $u_x$  and  $u_y$  are magnitudes of the particle velocities in the respective directions,  $\Delta t$  is the time step and  $\Delta x, \Delta y$  are the cell spatial dimensions. The Courant–Friedrichs–Lewy condition [16] is not the only constraint on simulation parameters, however, it is the most restrictive.

### 2.2. Atomic physics algorithm

The atomic physics algorithm utilises a superconfiguration approach to calculate atomic scattering factors in the EUV and X-ray for partially ionised plasmas. Detailed level structure is initially obtained by using the Flexible Atomic Code (FAC) [17] to solve the radial wave equation. This structure is post-processed to group energetically similar levels into ‘supershells’, where the average energy,  $\langle E \rangle_{SS}$  is weighted by the degeneracy ( $g_m$ ) and given by

$$\langle E \rangle_{SS} = \frac{\sum_m g_m E_m}{\sum_m g_m}, \quad (2)$$

where  $E_m$  is the energy of a single detailed level.

Ionisation and excited level populations are determined assuming local thermodynamic equilibrium, an assumption which is justified on hydrodynamic timescales of  $> ps$ , as the highly non-equilibrated plasma initially created equilibrates on the order of 10 s of fs [18]. Photoionisation cross-sections for each ionisation stage and superconfiguration level are calculated assuming a  $E^{-3}$  photon energy dependence, and a configuration specific constant ( $A(n, Z)$ ) determined using data from FAC. This approximation allows for an analytical solution to the Kramers–Kronig relation where the atomic scattering factor  $f_1^0(E)$  is given by

$$f_1^0(E) = Z^* + \frac{1}{\pi r_e h c} \left( \sum_Z \sum_n \frac{A(n, Z)}{2E^2} \log \left( \left| 1 - \frac{E^2}{E_{i,n}^2} \right| \right) \right), \quad (3)$$

where  $Z^*$  is the number of bound electrons,  $Z$  is the ionisation stage,  $n$  is the supershell number,  $E$  is the photon energy and  $E_{i,n}$  is the binding energy of an electron in supershell  $n$  of an ion with charge  $Z$ . The time averaged effects of the ionisation potential

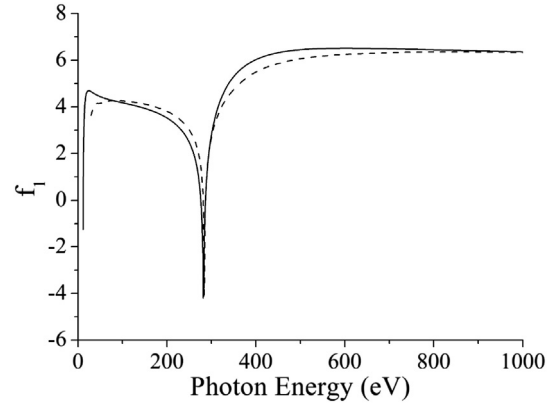


**Fig. 1.** Scattering factor,  $f_1$ , for cold, solid carbon as a function of photon energy. A comparison is made between our algorithm (solid line) and data from the Centre for X-ray Optics (CXRO) at Lawrence Berkeley National Laboratory (dashed line).

depression is accounted for in the binding energy,  $E_{i,n}$ , using the Stewart–Pyatt model [19,20]. Our refractive index model has shown reasonable agreement with data from the CXRO for cold, solid carbon, as is shown in Fig. 1, however, it is worth noting that the  $E^{-3}$  approximation breaks down for materials with  $Z \geq 13$ , especially in the energy region of  $E < 100$  eV.

The atomic physics algorithm is used to calculate the ion populations, free electron density and refractive index for each cell within the fluid code POLLUX and is updated for each time step. The populations and free electron density are used in the calculation of the laser absorption as outlined previously [21] and the refractive index is calculated to simulate the effect of the expanding plasma on the path of the laser pulse. As the free electron approximation for the refractive index is not valid in the EUV, the value of  $f_1^0(E)$  from Eq. (3) is used to calculate the real component of the refractive index. The refractive index is input into the ray tracing routine of POLLUX for each time step.

## 3. Results and discussion

Fig. 2 indicates the EUV laser induced ablation, with the laser incident from right to left irradiating a planar target with surface at  $x = 0$ . Fig. 2(a) and (b) show the ablation profiles for a capillary discharge laser, with photon energy 26 eV, irradiance of  $5 \times 10^9$  W cm $^{-2}$  and focal spot diameter (FWHM) of 500 nm after (a) 1 pulse and (b) 4 pulses. A depth of 4.2  $\mu m$  is ablated after 4 pulses with a lateral hole size of 1.3  $\mu m$  (FWHM). Fig. 2(c) and (d) show how the ablation profile changes as the focal spot diameter is reduced, approaching the diffraction limit. For a focal spot diameter of 200 nm, Fig. 2(c) and (d) show the ablation profiles after (c) a single pulse and (d) two pulses for an irradiance of  $5 \times 10^9$  W cm $^{-2}$ . After the second pulse, an ablated depth of 2.4  $\mu m$  is observed with a lateral hole size of 644 nm (FWHM). This indicates the potential of this technology for meso-scale (100 nm–1  $\mu m$ ) machining and the capability of the computational algorithms to optimise the ablative characteristics for specific applications. By comparing simulation results with ablation profiles obtained experimentally via atomic force microscopy, the code has been benchmarked using realistic focusing conditions and these results have been published in Refs. [21,22].

It is observed that plasma refractive index effects become significant at irradiances greater than  $1 \times 10^{10}$  W cm $^{-2}$ , resulting in the beam both self-focusing and diverging in different regions of the produced plasma. For this reason an efficient, temperature-dependent model for the atomic scattering factors is required to

Download English Version:

<https://daneshyari.com/en/article/8133548>

Download Persian Version:

<https://daneshyari.com/article/8133548>

[Daneshyari.com](https://daneshyari.com)